The Journal of Engineering

The 2nd 2018 Asian Conference on Artificial Intelligence Technology (ACAIT 2018)

IET Journals
The Institution of Engineering and Technology

New microscopic image sequence-driven cell deformation model

eISSN 2051-3305
Received on 19th July 2018
Accepted on 26th July 2018
E-First on 2nd October 2018
doi: 10.1049/joe.2018.8281
www.ietdl.org

Fuyun He[1,2], F. Jiang[1] ✉, Yanyan Jiang[1], Sai Ho Ling[3]

[1]*College of Electronic Engineering, Guangxi Normal University, Guilin, People's Republic of China*
[2]*State Key Laboratory for the Chemistry and Molecular Engineering of Medicinal Resources (Guanxi Normal University), Ministry of Education of China, People's Republic of China*
[3]*Faculty of Engineering and IT, University of Technology, Sydney, Australia*
✉ *E-mail: fjiang@gxnu.edu.cn*

Abstract: It is of great significance that making quantitative description and analysis of the cell morphological change to explore physiological or pathological status of the life. To achieve the cells morphological changes of quantitative description, the authors constructed a cell deformation model based on microscopic image sequence here. Based on the graph regularisation and structured matrix decomposition, the high-dimensional shape space is represented by the linear combination of the low-dimension subshape space, so that the authors get a quantitative indicator which represents the degree of cell deformation–deformation factor. In order to verify the validity of the authors' model, a deformation feature extraction experiment was performed on three groups of stem cell image sequence with different deformation degree. Compared with other three common quantitative methods of deformation, the authors' model describes the cell morphological changes more comprehensively, and has better adaptability and stability for describing the diversity of cell movements.

1 Introduction

Cell morphology is an intuitive manifestation of the physiological characteristics of life entity, and it is of great significance and broad application prospect to quantitatively describe and analyse the relationship between cell morphological changes and physiological and pathological processes of the human body [1]. In living cells, the dynamic change of morphology can reflect the physiological changes of organism. The effects of drugs or certain pathological processes, such as drug screening, wound healing, and proliferation of cancer cells, can cause cell morphological changes [2]. Therefore, the cell deformation model based on microscopic image sequences is more helpful to reveal the intrinsic relationship between cell morphological changes and physiological activities [3].

Cell morphological analysis is an effective tool to solve cell informatic problems, the quantitative characteristics of which include geometrical shape, strength, and texture. Paluch and Heisenberg [4] had discussed the morphological characteristics during cell growth, division apoptosis processes. Moreover, Keren *et al.* [5] had proposed the biochemical and biophysical models of fish corneal cells to quantitatively analyse cell morphological changes and kinematic velocity. Mogilner and Keren [6] had studied the diversity of dynamic behaviour of stromal cells in different environments and under motion mode. In addition, Jakob *et al.* [7] had analysed the degree of DNA damage through computer vision technique. Xiong and Iglesias [8] had given a detailed summary of all methods for analysing cell morphological changes, and suggested that cell morphological changes were the external characterisation of cellular chemotaxis and function.

A single shape feature descriptor based on target cell region extraction has been widely used, such as perimeter, area, eccentricity, roundness, and other scalar characteristics. High-order shape feature descriptors, such as Fourier descriptors, moments, and so on, describe Fuin, which can well depict spatial information of various shapes in many research work; however, the study of global feature descriptors for the morphological changes of target cells in image sequences/videos is relatively less. Therefore, based on microscopic image sequences, the cell deformation factors are extracted, and the dynamic changes are quantitatively described and analysed.

2 Cell deformation model

We assume that $\boldsymbol{X}_k \in \mathbb{R}^{N\times 2}$ stands for the coordinate matrix of N vertexes on target cellular outline, $\{X_1, X_2, \ldots, X_K\}$ suggests the coordinate set of all vertexes on K target cellular outlines in a cellular image sequence. Meanwhile, each line of $\boldsymbol{X}_k$ corresponds to the two-dimensional coordinates of a vertex, and the vertices in $\{X_1, X_2, \ldots, X_K\}$ of the same line number were homologous. In addition, $\boldsymbol{X}_k = \mathrm{vec}(X_k) \in \mathbb{R}^{2N}$ represented the column vector $\boldsymbol{X}_k$ from converting the matrix $\boldsymbol{X}_k$ with $2N$ dimension, and the combination of K $\boldsymbol{X}_k$ was expressed as $\boldsymbol{X} = [X_1, \ldots, X_K] \in \mathbb{R}^{2N\times K}$.

In order to make full use of the relationship between vertices, a weighted directed graph is $G = (\nu, \xi, \omega)$ is used to characterise the correlation between vertices [9], where $\nu = \{1, \ldots, N\}$ represents the vertex set, $\xi = \{1, \ldots, N\}^2$ is the edge set, and $\omega \in \mathbb{R}_{\xi}^{+}$ represents the weight. The weight ω_{e} of the edge $e = (i, j) \in \xi$, $i \neq j$ indicates the correlation between vertices i and j. The smaller ω_{e} indicates that the correlation between i and j is smaller.

Cellular outline variation pattern in the deformation factor matrix $\boldsymbol{\Phi} \in \mathbb{R}^{2N\times M}$ is defined as M most significant eigenvectors in the covariance matrix $\boldsymbol{C} = (\boldsymbol{X}\boldsymbol{X}^{\mathrm{T}}/K)$ of cell sample. Therefore, the vertex coordinate vector $\boldsymbol{X}_k$ of each target cellular outline could be expressed in the linear form

$$\boldsymbol{X}_k = \boldsymbol{\Phi}\alpha_k \tag{1}$$

where the linear coefficient $\alpha_k \in \mathbb{R}^M$.

3 The model solution

To solve the optimisation of deformation factor $\boldsymbol{\Phi}$ in target cellular outline sequence is to search for deformation factor $\boldsymbol{\Phi} = [\Phi_1, \ldots, \Phi_M]$ with the greatest significance as well as the linear coefficient $A = [\alpha_1, \ldots, \alpha_K] \in \mathbb{R}^{M\times K}$ based on a certain method in the presence of all known outline vertex coordinates X. In this way, the deviation between target cellular outline sequence

is reconstructed using formula (2) and the original target cellular outline sequence could be minimised

$$X' = (\boldsymbol{\Phi})_{2N\times M}(A)_{M\times K} \tag{2}$$

In practical applications, we set $M<2N$, the sparsity of the deformation factor $\boldsymbol{\Phi}$ is indicated to some extent.

To decompose $\boldsymbol{\Phi}$ and A from X, we adopted the loss function based on square Frobenius-norm to convert the matrix decomposition problem into the following optimisation problem

$$\min_{\boldsymbol{\Phi},A} \| X-\boldsymbol{\Phi}A \|_F^2 + \Omega(\boldsymbol{\Phi},A) \tag{3}$$

where $\Omega(\boldsymbol{\Phi},A)$ represents the applying of regularisation term constraint on $\boldsymbol{\Phi}$ and A.

For solving the above optimisation problem, it is assumed that the optimisation process is based on compact set and the change of adjacent vertices satisfies the smoothness constraint. Therefore, the introduction of regular entry further ensures the sparsity of the deformation factor $\boldsymbol{\Phi}$. Based on the decomposition norm, the formula (3) can be further represented as

$$\min_{\boldsymbol{\Phi},A} \| X-\boldsymbol{\Phi}A \|_F^2 + \lambda\sum_{m=1}^{M} \| \boldsymbol{\Phi}_m \|_{\boldsymbol{\Phi}} \| (A_{m,})^{\mathrm{T}} \|_A \tag{4}$$

where $\| \cdot \|_{\boldsymbol{\Phi}}$ and $\| \cdot \|_A$ represent the combined vector norm. For $y\in\mathbb{R}^K$ and $z\in\mathbb{R}^{2N}$, $\| \cdot \|_{\boldsymbol{\Phi}}$ and $\| \cdot \|_A$ are, respectively, defined as

$$\| y \|_A = \lambda_A \| y \|_2 \tag{5}$$

$$\| z \|_{\Phi} = \lambda_1 \| z \|_1 + \lambda_2 \| z \|_2 + \lambda_G \| \boldsymbol{E}z \|_2 \tag{6}$$

where the ℓ_1 norm is used to obtain the sparsity of the deformation factor $\boldsymbol{\Phi}$.

The third item in formula (6) represents the weighted directed graph-based ℓ_2 norm, which has applied smooth constraint in each factor. Based on the weighted directed graph-based incidence matrix, and $\| \boldsymbol{E}(z) \|_2$ stood for

$$\| \boldsymbol{E}z \|_2 = \sqrt{\sum_{d\in\{0,N\}}\sum_{(i,j)=e_p} \omega_{e_p}\left(z_{d+i}-z_{d+j}\right)^2} \tag{7}$$

where $\| \boldsymbol{E}(\cdot) \|_2^2$ indicated the regularisation terms in Laplace graph [10]. Matrix $\boldsymbol{E}$ is the disperse gradient operator, which could be represented as $\boldsymbol{E} = I_2 \otimes \boldsymbol{E}'$, while $\boldsymbol{E}'$ was expressed as

$$\boldsymbol{E}'_{pq} = \begin{cases} \sqrt{\omega_{e_p}} & \text{if } (q=i) \text{ for } \left(e_p=(i,j)\right) \\ -\sqrt{\omega_{e_p}} & \text{if } (q=j) \text{ for } \left(e_p=(i,j)\right) \\ 0 & \text{otherwise} \end{cases} \tag{8}$$

Meanwhile, $\boldsymbol{E}'_{pq}$ suggested the weighted incidence matrix of weighted directed graph $G=(\nu,\xi,\omega)$,and $p=1,\ldots,|\xi|,\ q=1,\ldots,N$, $e_p\in\xi$ is the pth edge of the graph G.

4 Cell deformation quantitative

The deformation of the contour of cell image sequence can reflect the corresponding physiological or pathological phenomena of the organism. Therefore, if we can effectively extract the characteristics of the morphological changes of the cell images and make them relate to the physiological or pathological phenomena of the organism, the parameters describing the dynamic characteristics of cell shape can be applied to the identification and classification of the cell lesion pattern.

Stem cell image sequences were derived from the pluripotent stem cell microscopic image sequence database of VISLab (Visualization and Intelligent Systems Laboratory), University of California, and Riverside. Such database included stem cell image sequences of three different quality categories. Fig. 1 shows the different image frames of the stem cell image sequence, which were the 1st, 25th, 50th, and 75th image frames of that image sequence from the left to the right in order.

The image sequences of the stem cells were firstly taken as denoising, deblurring processing, cell tracking, and cell segmentation, and binary image sequences were obtained. Then, the contour shapes of these image sequences are extracted, as shown in the first line of Fig. 2, which shows the result of reconstructing the cell shape sequence after the deformation factor and linear coefficient of the cell deformation sequence obtained by using four different decomposition methods. The first line is the true cell image sequence of the contour shape (from left to right in the order of cell image sequence of the 1st, 25th, 50th, 75th frames), the second line is used in the proposed method to reconstruct the cell shape sequence, the third line is used the method of [9] to reconstruct the cell shape sequence, the fourth line is used the method of [10] to reconstruct the cell shape sequence, and the fifth line is used the method of [11] to reconstruct the cell shape sequence. Compared with the other three methods, our method with the reconstruction effect of the cell shape sequence is relatively good from the perspective of subjective visual contrast.

To measure the quantitative difference among different methods in reconstructing cell morphological sequence, the error results of each method in reconstructing cellular outline morphological sequence are shown in Table 1. As could be observed from data in Table 1, the reconstruction error of each method for the outline morphology of each frame in cell image slightly fluctuated within the range of average reconstruction error; with the greatest fluctuation is 0.0049. This suggested an ideal reconstruction consistency of all methods. Notably, the sequence reconstruction error values of the proposed method, methods in [9, 10] and [11], were 0.1281, 0.1525, 0.2063, and 0.2960, respectively. Thus, it could be determined that the reconstruction effect of the proposed method was superior to that of the other three methods.

5 Conclusion

In this paper, based on microscopic image sequences, the morphological changes of cells are more accurately quantified, and the sequence deformation factors are more suitable for the dynamic description of cell morphological changes than the usual static shape description methods. The method presented in this paper has a good distinction between different degrees of cell deformation. Quantitative description of cell morphological changes combined with the physiological characteristics of cells. The relationship between cell physiology and morphological changes can be established, which is very important to explore the physiological or pathological process of cells. At the same time, it can be used to

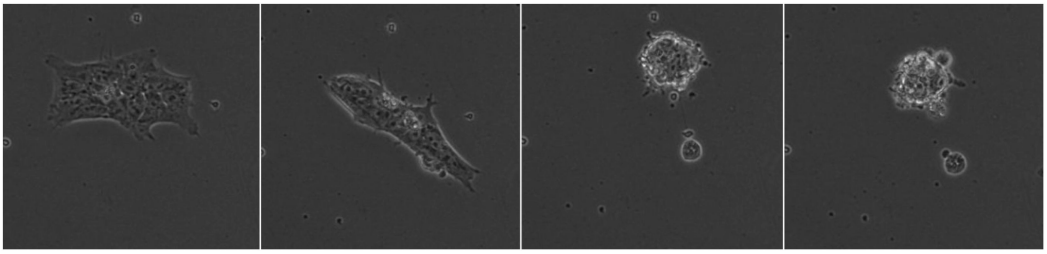

Fig. 1 *Image frames of stem cell image sequence*

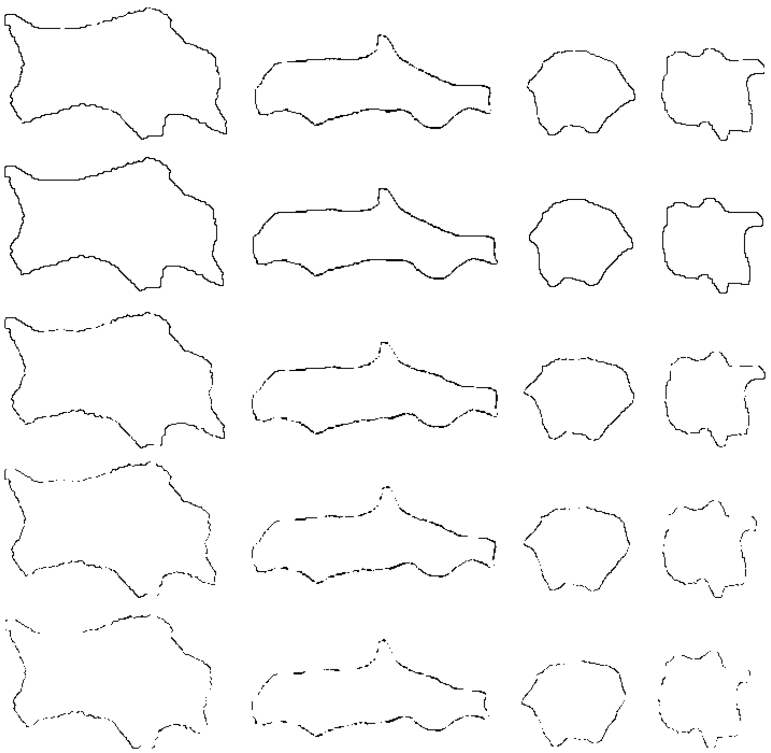

Fig. 2 *Results of reconstructing the deformation contour of stem cell image sequences with different methods*

Table 1 Reconstructing errors of deformation contour of stem cell image sequences with different methods

Frames/method	Ours	Ref. [9]	Ref. [10]	Ref. [11]
1	0.1272	0.1511	0.2142	0.3016
25	0.1239	0.1602	0.2095	0.2974
70	0.1276	0.1541	0.1999	0.2951
75	0.1336	0.1445	0.2063	0.2899
average	0.1281	0.1525	0.2075	0.2960

assist in the detection of abnormal morphological cells, such as cancer cells, immune rejection cell, and so on, which can provide an objective reference for early diagnosis.

6 Acknowledgments

The project was funded by Key Laboratory for the Chemistry and Molecular Engineering of Medicinal Resources (Guangxi Normal University), Ministry of Education of China (CMEMR2015-B11), and the 2017 basic ability promotion project for middle-aged and young teachers in colleges and universities in Guangxi (2017KY0079). This work was partially supported by the Guangxi Program (F-KA16016), National Natural Science Foundation of China (61762018, 11562004) and the Colleges and Universities Key Laboratory of Intelligent Integrated Automation, Guilin University of Electronic Technology, China (GXZDSY2016-03). The research fund of Guangxi Key Lab of Multi-source Information Mining & Security (18-A-02-02).

7 References

[1] Pretorius, A.J., Khan, I.A., Errington, R.J.: 'A survey of visualization for live cell imaging', *Comput. Graph. Forum*, 2017, **36**, pp. 46–63

[2] Mohan, K., Luo, T., Robinson, D.N., *et al.*: 'Computational model for cell shape regulation through mechanosensing and mechanical feedback', *Biophys. J.*, 2014, **106**, pp. 378a–378a

[3] Ghosh, N.: '*Video bioinformatics methods for analyzing cell dynamics: a survey. Video bioinformatics*' (Springer International Publishing, Basel, 2015)

[4] Paluch, E., Heisenberg, C.P.: 'Biology and physics of cell shape changes in development', *Curr. Biol.*, 2009, **19**, (1), pp. 790–799

[5] Keren, K., Pincus, Z., Allen, G.M., *et al.*: 'Mechanism of shape determination in motile cells', *Nature*, 2008, **453**, (719), p. 475

[6] Mogilner, A., Keren, K.: 'The shape of motile cells', *Curr. Biol.*, 2009, **19**, (1), p. R762

[7] Jakob, B., Splinter, J., Durante, M., *et al.*: 'Live cell microscopy analysis of radiation-induced DNA double-strand break motion', *Proc. Natl Acad. Sci. USA*, 2009, **106**, (9), pp. 3172–3177

[8] Xiong, Y., Iglesias, P.A.: 'Tools for analyzing cell shape changes during chemotaxis', *Integr. Biol. Quant. Biosci. Nano Macro*, 2010, **2**, (11-1), pp. 561–567

[9] Feng, C. M., Liu, J. X., Gao, Y. L., *et al.*: 'A graph-Laplacian PCA based on L1/2-norm constraint for characteristic gene selection'. IEEE Int. Conf. on Bioinformatics and Biomedicine, Shenzen, China, December 2016, pp. 1795–1799

[10] Bouwmans, T., Zahzah, E. H.: 'Robust PCA via principal component pursuit: a review for a comparative evaluation in video surveillance', *Comput. Vis. Image Underst.*, 2014, **122**, pp. 22–34

[11] Last, C., Winkelbach, S., Wahl, F. M., *et al.*: 'A locally deformable statistical shape model', in '*International Workshop on Machine Learning in Medical Imaging*' (Springer, Berlin, 2011), pp. 51–58